Victor Iliev Rizov

DELAMINATION STUDY OF INHOMOGENEOUS BEAMS WITH RECTANGULAR CROSS-SECTION EXHIBITING RELAXATION UNDER TORSION

RASLOJAVANJE NEHOMOGENIH NOSAČA PRAVOUGAONOG POPREČNOG PRESEKA SA POJAVOM RELAKSACIJE POD DEJSTVOM UVIJANJA

Originalni naučni rad / Original scientific paper
UDK /UDC:

Rad primljen / Paper received: 11.01.2022

Adresa autora / Author's address:
University of Architecture, Civil Engineering and Geodesy, Department of Technical Mechanics, Sofia, Bulgaria
email: v_rizov_fhe@uacg.bg

Keywords
- relaxation
- inhomogeneous beam
- delamination
- torsion

Ključne reči
- relaksacija
- nehomogeni nosač
- raslojavanje
- uvijanje

Abstract

Inhomogeneous beam structures of rectangular cross-section loaded in torsion are widely used in various load-bearing engineering applications. Delamination is one of the factors which have significant influence on the integrity and reliability of these beam structures. In many load-bearing structures, the inhomogeneous beams exhibit relaxation behaviour in their life-time. Therefore, this paper studies the delamination in beams under torsion considering the relaxation of stresses and its effect on the strain energy release rate. The beam has two longitudinal vertical layers. The delamination is between the layers. The free ends of the crack arms are loaded in torsion. The angles of twist are kept constant with time in order to induce relaxation behaviour. An analysis of the time-dependent compliance of the beam under torsion is performed to derive the strain energy release rate. The J-integral method is applied to verify the solution of the time-dependent strain energy release rate. The influence of various parameters on the strain energy release rate is assessed by using the derived solution.

Izvod

Konstrukcije nehomogenih nosača pravougaonog poprečnog preseka opterećeni na uvijanje se u većoj meri primenjuju u nosećim inženjerskim konstrukcijama. Raslojavanje je jedan od faktora sa značajnim uticajem na integritet i pouzdanost ovih nosača. U mnogim nosećim konstrukcijama, u nehomogenim nosačima se javlja relaksacija u toku radnog veka. Stoga se u radu proučava raslojavanje u nosačima pod dejstvom uvijanja sa razmatranjem relaksacije napona i njen uticaj na brzinu oslobađanja deformacione energije. Nosač ima dva vertikalna podužna sloja. Slobodni krajevi površina prsline su opterećeni na uvijanje. Uglovi uvijanja su konstantni u vremenu kako bi se izazvala pojava relaksacije. Izvedena je analiza vremenski zavisne popustljivosti nosača opterećenog na uvijanje kako bi se odredila brzina oslobađanja deformacione energije. Primenjen je J-integral za verifikaciju rešenja vremenski zavisne brzine oslobađanja deformacione energije. Procenjen je uticaj raznih parametara na brzinu oslobađanja deformacione energije korišćenjem dobijenog rešenja.

INTRODUCTION

Continuously inhomogeneous material is a type of structural material whose properties are continuous functions of one or more coordinates in the solid. Different kinds of continuously inhomogeneous materials exist. Currently, one of the most used continuously inhomogeneous materials is the functionally graded material /1-3/. The concept of functionally graded materials was developed first in Japan in the 1980s. Functionally graded materials are inhomogeneous composites which represent combinations of two or more constituent materials. Continuous change of macroscopic properties of functionally graded materials in the structural member is obtained by varying the composition of constituent materials along one or more spatial coordinates with a specific gradient during the manufacturing process /4-7/. The microstructure of functionally graded materials can be tailored technologically in order to meet various performance requirements and to enhance the reliability and durability of engineering structures /8-11/. High-performance functionally graded materials are widely used for manufacturing structural members and components in various areas of modern engineering (aeronautics, car industry, nuclear reactors, etc).

The study of delamination in continuously inhomogeneous (functionally graded) materials is an important topic of the contemporary fracture mechanics since delamination fracture is a common failure mode of engineering structures made of these materials. It is obvious that knowledge of the delamination provides the basis for the design of safe and reliable continuously inhomogeneous load-bearing structures /12/. Analysing delamination behaviour of structural members of various geometries subjected to different loading conditions is of great significance for avoiding the delamination type of failure in engineering applications.

The aim of this paper is to analyse the delamination in a continuously inhomogeneous beam structure of rectangular cross-section loaded in torsion. The beam exhibits relaxation behaviour that is taken into account in the delamination analysis. The beam is made of two longitudinal vertical layers continuously inhomogeneous in longitudinal direction. A delamination crack is located between layers. The angles of

twist of the free ends of the crack arms are fixed in order to induce relaxation of stresses. The strain energy release rate is derived by analysing the compliance of the beam under relaxation. The method of the J-integral is applied to verify the strain energy release rate. It should be mentioned that inhomogeneous beams loaded in torsion are widely used in various load-bearing structural applications. However, the delamination analyses of structures loaded in torsion deal usually with beams of circular cross-section, /13, 14/. Therefore, the paper fills up this emptiness in delamination analyses by considering inhomogeneous beams of rectangular cross-section subjected to torsion.

DELAMINATION ANALYSIS

Consider the beam structure depicted in Fig. 1.

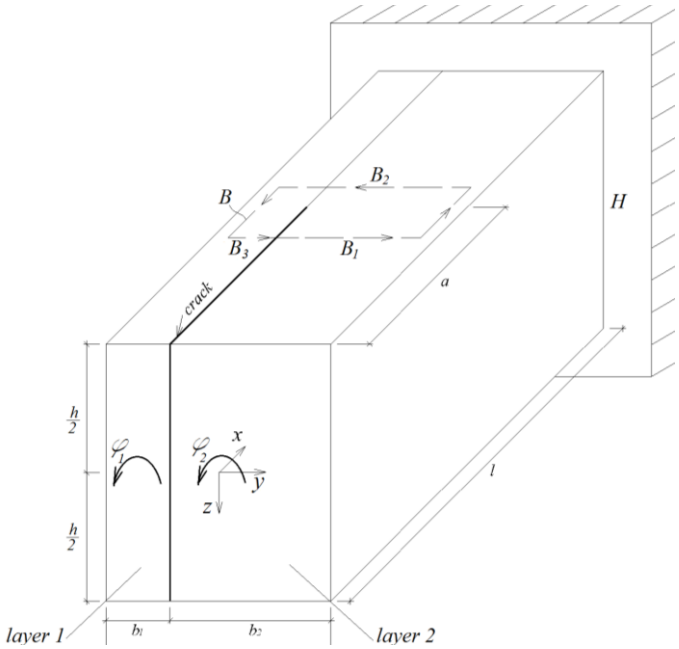

Figure 1. Viscoelastic inhomogeneous beam structure of rectangular cross-section with a delamination crack.

The width, thickness, and length of the beam are b, h, and l, respectively. The beam is made of two adhesively bonded longitudinal vertical layers of widths, b_1 and b_2. There is a delamination crack of length, a, between layers. The beam is clamped in section, H. The two layers are made of different materials. The two crack arms are loaded in torsion, so as the angles of twist, φ_1 and φ_2, of the free ends of the crack arms do not change with time. Under these loading conditions, the beam exhibits relaxation behaviour, i.e. stresses decrease with time while strains remain constant.

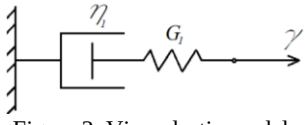

Figure 2. Viscoelastic model.

The relaxation behaviour of layer 1 is treated by using the viscoelastic mechanical model depicted in Fig. 2. The shear modulus of the spring and the coefficient of viscosity of the dashpot are denoted by G_1 and η_1, respectively (Fig. 2). The model is under a constant shear strain, γ. The constitutive law of the model is written as /15/,

$$\tau = G_1 \gamma e^{-\frac{G_1 t}{\eta_1}}, \tag{1}$$

where: τ is shear stress; t is time. Equation (1) describes the relaxation of stresses in layer 1 and is applied also for modelling of stress relaxation in layer 2 of the beam (Fig. 1). For this purpose, τ, γ, G_1, and η_1, are replaced with τ_R, γ_R, G_{1R}, and η_{1R}, respectively. Here, τ_R, γ_R, G_{1R}, and η_{1R} are shear stress, strain, shear modulus, and coefficient of viscosity in layer 2, respectively.

The time-dependent shear modulus, $G_*(t)$, for the viscoelastic model in Fig. 2 is defined as

$$G_*(t) = \frac{\tau(t)}{\gamma}. \tag{2}$$

By substituting Eq.(1) in Eq.(2), one obtains

$$G_*(t) = G_1 e^{-\frac{G_1 t}{\eta_1}}. \tag{3}$$

Equation (3) is used also to determine the time-dependent shear modulus, $G_{*R}(t)$, of beam layer 2 by replacing $G_*(t)$, G_1, and η_1 with $G_{*R}(t)$, $G_{1R}(t)$, and η_{1R}, respectively.

The material in both layers is continuously inhomogeneous in longitudinal direction of the beam. The distribution of material properties in layer 1 along the length of the beam is expressed by the following functions:

$$G_1 = G_{1n} + \frac{G_{1m} - G_{1n}}{l^f} x^f, \tag{4}$$

$$\eta_1 = \eta_{1n} + \frac{\eta_{1m} - \eta_{1n}}{l^g} x^g, \tag{5}$$

where: $$0 \le x \le l. \tag{6}$$

In Eqs.(4), (5), and (6), x is the longitudinal centroidal axis of the beam; G_{1n} and G_{1m} are values of G_1 in the free end and in the clamping of the beam; f is a parameter controlling the distribution of the shear modulus along the beam length. The values of η_1 in the free end and in the clamping are denoted by η_{1n} and η_{1m}, respectively. The distribution of η_1 along the beam length is controlled by parameter g. Equations (4) and (5) are used also to describe the variation of the shear modulus and the coefficient of viscosity in layer 2 of the beam. For this purpose, G_{1n}, G_{1m}, f, η_{1n}, η_{1m}, and g are replaced by G_{1Rn}, G_{1Rm}, s, η_{1Rn}, η_{1Rm}, and p, respectively.

Strain energy release rate, G, for the delamination (Fig. 1) is derived by analysing the compliance of the beam with taking into account relaxation behaviour. For this purpose, the stress-strain-time constitutive law Eq.(1) is applied. The beam compliances, C_1 and C_2, are obtained as

$$C_1 = \frac{\phi_1}{T_1}, \tag{7}$$

$$C_2 = \frac{\phi_2}{T_2}, \tag{8}$$

where: T_1 and T_2 are /torsion moments at free ends of the left-hand and right-hand crack arms, in respect. By applying the compliance method, the strain energy release rate is found as

$$G=\frac{T_1^2}{2h}\frac{dC_1}{da}+\frac{T_2^2}{2h}\frac{dC_2}{da}. \quad (9)$$

The angles of twist of free ends of the crack arms are presented as functions of crack length by applying the integrals of Maxwell-Mohr. In this manner, one derives,

$$\phi_1=\int_0^a\frac{T_1}{G_*I_1}dx+\int_a^l\frac{T_3}{G_{*D}I}dx, \quad (10)$$

$$\phi_2=\int_0^a\frac{T_2}{G_{*R}I_2}dx+\int_a^l\frac{T_3}{G_{*D}I}dx, \quad (11)$$

where: T_3 is torsion moment in the un-cracked beam portion $a \le x \le l$, is found as

$$T_3=T_1+T_2. \quad (12)$$

Moments of inertia, I_1 and I_2, of cross-sections of the left-hand and right-hand crack arms under torsion involved in Eqs.(10) and (11) are calculated as, /16/,

$$I_1=\frac{b_1h^3}{3}-\left(\frac{4}{\pi}\right)^5\left(\frac{h}{2}\right)^4\sum_{i=1}^{\infty}\frac{\tanh(jb_1)}{(2i+1)^5}, \quad (13)$$

$$I_2=\frac{b_2h^3}{3}-\left(\frac{4}{\pi}\right)^5\left(\frac{h}{2}\right)^4\sum_{i=1}^{\infty}\frac{\tanh(jb_2)}{(2i+1)^5}, \quad (14)$$

where:
$$j=\frac{(2i+1)\pi}{h}. \quad (15)$$

The rigidity in torsion, $G_{*D}I$, of the un-cracked beam portion involved in Eqs.(10) and (11) is found by applying the following formula, /16/:

$$G_{*D}I=\frac{8}{3}(G_*b_1+G_{*R}b_2)\left(\frac{h}{2}\right)^3+\left(\frac{4}{\pi}\right)^5\left(\frac{h}{2}\right)^4\times$$
$$\times\sum_{i=0}^{\infty}\left[\frac{G_*^2\cosh(jb_2)+G_{*R}^2\cosh(jb_1)}{Q}-\frac{(G_*^2+G_{*R}^2)\cosh(jb_1)\cosh(jb_2)}{Q}\right]-$$
$$-\left(\frac{4}{\pi}\right)^5\left(\frac{h}{2}\right)^4G_*G_{*R}\sum_{i=0}^{\infty}\left\{\frac{\cosh(jb_1)+\cosh(jb_2)}{Q}-\frac{\cosh[j(b_1-b_2)]-1}{Q}\right\}, \quad (16)$$

where:

$$Q=(2i+1)^5\left[G_*\cosh(jb_2)\sinh(jb_1)+G_{*R}\cosh(jb_1)\sinh(jb_2)\right]. \quad (17)$$

It should be noted that G_* and G_{*R} in Eqs.(16) and (17) are determined by using Eq.(3).

Equations (10), (11), and (12) are solved with respect to T_1 and T_2. The result is,

$$T_1=\frac{\phi_1(\delta_2+\delta_3)-\phi_2\delta_2}{\delta_1\delta_3+\delta_2\delta_3+\delta_1\delta_2}, \quad (18)$$

$$T_2=\frac{\phi_1}{\delta_2}-\frac{(\delta_1+\delta_2)[\phi_1(\delta_2+\delta_3)-\phi_2\delta_2]}{\delta_2(\delta_1\delta_3+\delta_2\delta_3+\delta_1\delta_2)}, \quad (19)$$

where:
$$\delta_1=\int_0^a\frac{1}{G_*I_1}dx, \quad (20)$$

$$\delta_2=\int_a^l\frac{1}{G_{*D}I}dx, \quad (21)$$

$$\delta_3=\int_0^a\frac{1}{G_{*R}I_2}dx. \quad (22)$$

The integration in Eqs.(20), (21), and (22) is carried-out by using the MatLab® computer programme (it should be mentioned that quantities G_*, $G_{*D}I$, and G_{*R} are functions of x, since the two layers are continuously inhomogeneous along the beam length).

Finally, by substituting Eqs.(7), (8), (10), and (11) in Eq. (9), one derives,

$$G=\frac{T_1}{2h}\left(\frac{T_1}{G_*I_1}-\frac{T_3}{G_{*D}I}\right)+\frac{T_2}{2h}\left(\frac{T_2}{G_{*R}I_2}-\frac{T_3}{G_{*D}I}\right), \quad (23)$$

where: T_1 and T_2 are found by Eqs.(18) and (19), in respect. Dependency Eq.(12) is applied to obtain the torsion moment, T_3, involved in Eq.(23). Equation (23) can be used to calculate the strain energy release rate at various values of time.

The method of the J-integral /17/ is applied to verify the solution of the strain energy release rate Eq.(23). The integration is performed along contour B, shown by dashed line in Fig. 1. The solution of the J-integral is found as

$$J=J_{B_1}+J_{B_2}+J_{B_3}, \quad (24)$$

where: J_{B1}, J_{B2}, and J_{B3} are values of J-integral in segments B_1, B_2, and B_3, respectively.

In segment B_1, of the integration contour, the J-integral is expressed as

$$J_{B_1}=\int_{B_1}\left[u_{01}\cos\alpha_{B_1}-\left(p_{x_{B_1}}\frac{\partial u}{\partial x}+p_{y_{B_1}}\frac{\partial v}{\partial x}\right)\right]ds_{B_1}. \quad (25)$$

The expressions of J-integral in segments B_2 and B_3 are obtained as

$$J_{B_2}=\int_{B_2}\left[u_{02}\cos\alpha_{B_2}-\left(p_{x_{B_2}}\frac{\partial u}{\partial x}+p_{y_{B_2}}\frac{\partial v}{\partial x}\right)\right]ds_{B_2}, \quad (26)$$

and
$$J_{B_3}=\int_{B_3}\left[u_{03}\cos\alpha_{B_3}-\left(p_{x_{B_3}}\frac{\partial u}{\partial x}+p_{y_{B_3}}\frac{\partial v}{\partial x}\right)\right]ds_{B_3}, \quad (27)$$

respectively.

The average value of the J-integral along the crack front is derived as

$$J_{av}=\frac{1}{h}\int_0^h Jdz. \quad (28)$$

By combining Eqs.(25), (26), (27), and (28), one obtains

$$J_{av}=\frac{1}{h}\int_{-\frac{h}{2}}^{\frac{h}{2}}\left\{\int_{B_1}\left[u_{01}\cos\alpha_{B_1}-\left(p_{x_{B_1}}\frac{\partial u}{\partial x}+p_{y_{B_1}}\frac{\partial v}{\partial x}\right)\right]ds_{B_1}+\right.$$
$$+\int_{B_2}\left[u_{02}\cos\alpha_{B_2}-\left(p_{x_{B_2}}\frac{\partial u}{\partial x}+p_{y_{B_2}}\frac{\partial v}{\partial x}\right)\right]ds_{B_2}+$$
$$\left.+\int_{B_3}\left[u_{03}\cos\alpha_{B_3}-\left(p_{x_{B_3}}\frac{\partial u}{\partial x}+p_{y_{B_3}}\frac{\partial v}{\partial x}\right)\right]ds_{B_3}\right\}dz. \quad (29)$$

The MatLab® computer programme is used to solve the integrals in Eq.(29) at various values of time. The J-integral values obtained by Eq.(29) match the strain energy release rates calculated by applying Eq.(23) which confirms the correctness of the solution of the strain energy release rate.

NUMERICAL RESULTS

The numerical results are obtained by using the solution of the strain energy release rate.

The following data are used: b = 0.020 m; h = 0..030 m; l = 0.450 m; f = g = s = p = 0.8; φ_1 = 0.006 rad and φ_2 = 0.006 rad.

The variation of strain energy release rate with time is shown in Fig. 3 at three G_{1m}/G_{1n} ratios. It should be noted that the strain energy release rate and time in Fig. 3 are expressed in non-dimensional form by using formulae $G_N = G/(G_{1n}h)$ and $t_N = tG_{1n}/\eta_{1n}$, respectively.

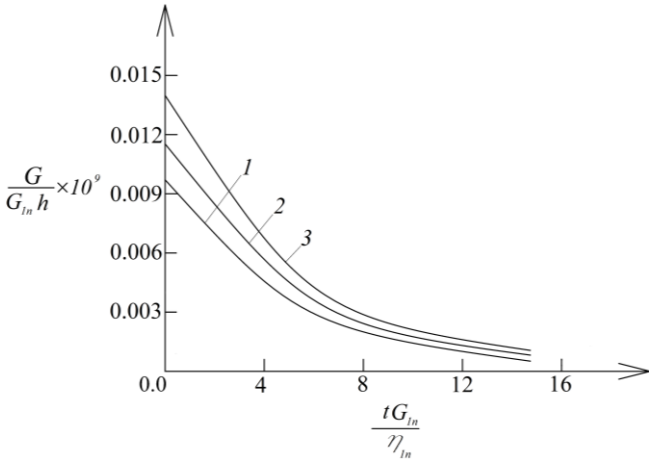

Figure 3. Strain energy release rate presented as a function of time (curve 1, at G_{1m}/G_{1n} = 0.5; curve 2, at G_{1m}/G_{1n} = 1.0; and curve 3, at G_{1m}/G_{1n} = 2.0).

It is evident from Fig. 3 that relaxation leads to reduction of the strain energy release rate with time. Also, the curves in Fig. 3 show that the strain energy release rate increases when G_{1m}/G_{1n} ratio increases.

The strain energy release rate is presented as a function of η_{1m}/η_{1n} ratio at three values of the angle of twist, φ_1, in Fig. 4. One can observe that when the angle of twist increases, the strain energy release rate increases too (Fig. 4). The increase of η_{1m}/η_{1n} ratio causes increase of the strain energy release rate (Fig. 4).

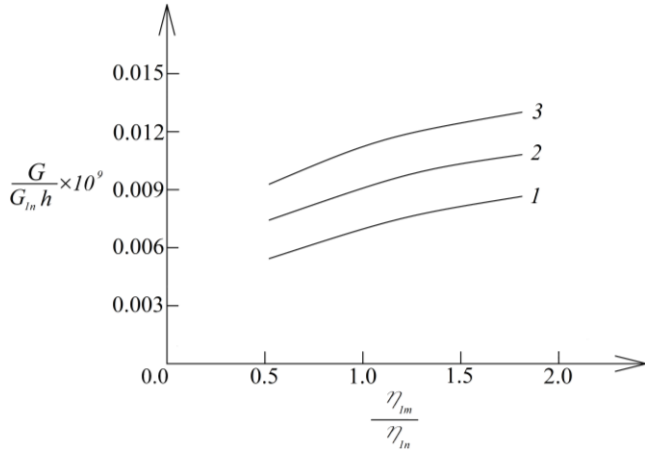

Figure 4. Strain energy release rate presented as a function of η_{1m}/η_{1n} ratio (curve 1, at φ_1 = 0.002 rad; curve 2, at φ_1 = 0.004 rad; and curve 3, at φ_1 = 0.006 rad).

The influence of G_{1Rn}/G_{1n} and η_{1Rn}/η_{1n} ratios on the strain energy release rate is illustrated in Fig. 5. It can be observed in Fig. 5 that increase of G_{1Rn}/G_{1n} and η_{1Rn}/η_{1n} ratios leads to increase of the strain energy release rate.

The influence of delamination length on strain energy release rate is also assessed. For this purpose, the strain energy release rate is presented as a function of *a/l* ratio at three G_{1Rm}/G_{1Rn} ratios in Fig. 6. The curves in Fig. 6 indicate that the strain energy release rate increases when *a/l* ratio increases. The increase of G_{1Rm}/G_{1Rn} ratio also causes increase of the strain energy release rate (Fig. 6).

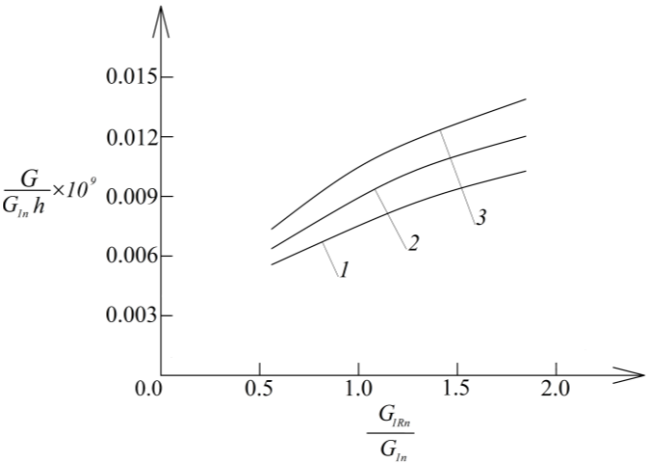

Figure 5. Strain energy release rate presented as a function of G_{1Rm}/G_{1n} ratio (curve 1, at η_{1Rn}/η_{1n} = 0.5; curve 2, at η_{1Rn}/η_{1n} = 1.0; and curve 3, at η_{1Rn}/η_{1n} = 2.0).

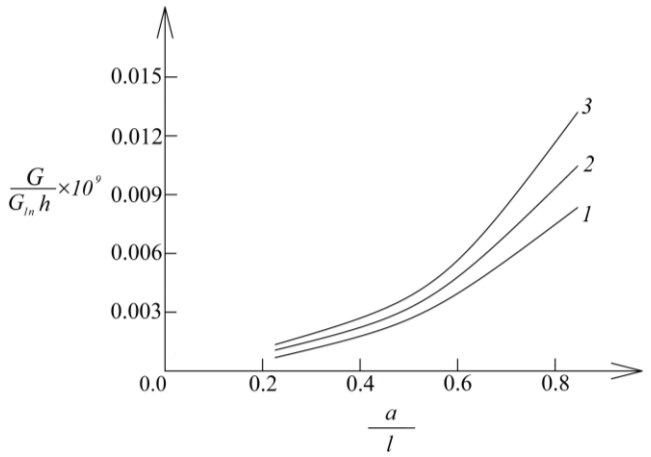

Figure. 6. Strain energy release rate presented as a function of *a/l* ratio (curve 1, G_{1Rm}/G_{1Rn} = 0.5; curve 2, G_{1Rm}/G_{1Rn} = 1.0; and curve 3, G_{1Rm}/G_{1Rn} = 2.0).

CONCLUSIONS

Delamination of inhomogeneous viscoelastic beam structure of rectangular cross-section loaded in torsion is analysed. The beam is made of two vertical longitudinal layers which are continuously inhomogeneous in the length direction. The influence of relaxation is studied. Conditions for relaxation of stresses in the beam structure are generated by fixing the angles of twist of the free ends of the crack arms. Solution of the time-dependent strain energy release rate is found by analysing the compliance of the beam under torsion with taking into account the relaxation behaviour. In order to verify the strain energy release rate, the delamination is investigated also by applying the method of the J-integral with considering the effects of relaxation. The obtained results indicate that the strain energy release rate is strongly influenced by the relaxation of stresses. The material inhomogeneity in longitudinal direction and the layered structure of the beam also have significant influence on the strain

energy release rate. It is found that the strain energy release rate increases when G_{1m}/G_{1n}, η_{1m}/η_{1n}, G_{1Rn}/G_{1n}, η_{1Rn}/η_{1n}, and G_{1Rm}/G_{1Rn} ratios increase. The increase of delamination length and the angles of twist also cause increase of the strain energy release rate.

REFERENCES

1. El-Galy, I.M., Saleh, B.I., Ahmed, M.H. (2019), *Functionally graded materials classifications and development trends from industrial point of view*, SN Appl. Sci. 1: 1378-1389. doi: 10.1007/s42452-019-1413-4
2. Hirai, T., Chen, L. (1999), *Recent and prospective development of functionally graded materials in Japan*, Mater Sci. Forum, 308-311(2): 509-514. doi: 10.4028/www.scientific.net/msf.308-311.509
3. Hedia, H.S., Aldousari, S.M., Abdellatif, A.K., Fouda, N.A. (2014), *New design of cemented stem using functionally graded materials (FGM)*, Biomed. Mater. Eng. 24(3): 1575-1588. doi: 10.3233/BME-140962
4. Neubrand, A., Rödel, J. (1997), *Gradient materials: An overview of a novel concept*, Zeit. f . Met. 88(1): 358-371.
5. Nikbakht, S., Kamarian, S., Shakeri, M. (2019), *A review on optimization of composite structures, Part II: Functionally graded materials*, Compos. Struct. 214: 83-102. doi: 10.1016/j.compstruct.2019.01.105
6. Gasik, M.M. (2010), *Functionally graded materials: bulk processing techniques*, Int. J Mater. Prod. Technol. 39(1-2): 20-29. doi: 10.1504/IJMPT.2010.034257
7. Suresh, S., Mortensen, A., Fundamentals of Functionally Graded Materials: Processing and Thermomechanical Behavior of Graded Metals and Metal-Ceramic Composites, IOM Communications Ltd., London, 1998.
8. Toudehdehghan, A., Lim, J.W., Foo, K.E., et al. (2017), *A brief review of functionally graded materials*, MATEC Web Conf. 131: 03010. doi: 10.1051/matecconf/201713103010
9. Yan, W., Ge, W., Smith, J., et al. (2016), *Multi-scale modeling of electron-beam melting of functionally graded materials*, Acta Mater. 115: 403-412. doi: 10.1016/j.actamat.2016.06.022
10. Saiyathibrahim, A., Subramaniyan, R., Dhanapl, P. (2016), *Centrifugally cast functionally graded materials - A review*, In: Int. Conf. on Systems, Science, Control, Communications, Eng. and Technology, Vol.02, pp.68-73.
11. Mahamood, R.M., Akinlabi, E.T., Functionally Graded Materials, Springer Cham, 2017. doi: 10.1007/978-3-319-53756-6
12. Rizov, V.I. (2018), *Delamination in multi-layered functionally graded beams - an analytical study by using the Ramberg-Osgood equation*, Struct. Integ. Life, 18(1): 70-76.
13. Rizov, V.I. (2019), *Non-linear fracture in bi-directional graded shafts in torsion*, Multidisc. Model. Mater. Struct. 15(1): 156-169. doi: 10.1108/MMMS-12-2017-0163
14. Rizov, V.I. (2021), *Inhomogeneous structural component with two lengthwise cracks - A nonlinear fracture analysis*, Struct. Integ. Life, 21(2): 157-162.
15. Rabotnov, Yu.N., Creep of Structural Members, Nauka Moscow, 1966. (in Russian)
16. Arutunian, N.Kh., Abramian, B.L., Torsion of Elastic Solids, Fitzmatgiz, Moscow, 1963. (in Russian)
17. Broek, D., Elementary Engineering Fracture Mechanics, 2nd Ed., Springer Dordrecht, 1986.